

# Direct evidence for an inelastic neutron acceleration process on $^{177m}\text{Lu}(n,n')$ reaction

O. Roig, V. Méot, B. Rossé, G. Bélier, J-M. Daugas, and P. Morel  
*CEA DAM DIF, F-91297 Arpajon, FRANCE*

A. Menelle  
*CEA DSM LLB, F-91191 Gif-sur-Yvette, FRANCE and  
CNRS INP UMR12, F-91191 Gif-sur-Yvette, FRANCE*

A. Letourneau, D. Doré, and Ch. Veyssière  
*CEA DSM IRFU, F-91191 Gif-sur-Yvette, FRANCE*

(Dated: January 3, 2011)

The inelastic neutron acceleration (INNA) cross section on the long-lived metastable state of  $^{177}\text{Lu}$  has been measured from a new isomeric target using a direct method. High energy neutrons have been detected using a specially designed setup and a cold neutron beam extracted from the ORPHEE reactor facility in Saclay. The results confirm the high cross section value previously published for INNA cross section on the  $^{177m}\text{Lu}$ .

PACS numbers: 25.40.Fq, 25.40.Lw, 25.60.Dz, 27.70.+q  
Keywords: INNA, capture, Lutetium isotopes

## I. INTRODUCTION

Super-elastic neutron scattering, also called inelastic neutron acceleration (INNA), occurs during the collision of a neutron with an excited nucleus. In this reaction, the nucleus transfers some of its excitation energy to the scattered neutron. Predicted since 1959 [1], this process was observed twenty years later on two isomeric nuclei,  $^{152m}\text{Eu}$  [2] and  $^{180m}\text{Hf}$  [3]. The effect of this neutron induced de-excitation is known in nuclear astrophysics to take place in the s-process nucleosynthesis [4–6]. Thanks to the usually high cross section of the thermal neutron interaction, such a process could be used to induce a fast de-excitation of an isomer. The 160-day 23/2- isomer in  $^{177}\text{Lu}$  ( $E_x = 970$  keV) is a good candidate to observe the inelastic neutron acceleration reaction. The production of an easy to handle target has been undertaken several times at the Laüe Langevin Institute (ILL) [7, 8]. The high value,  $(258 \pm 58)$  b, of the thermal INNA reaction cross section for  $^{177m}\text{Lu}$  has been deduced indirectly from burn-up [9] and capture cross sections [10]. The radiative capture cross section has been extracted under two reasonable hypothesis : (i) the  $^{177m}\text{Lu}(n,\gamma)^{178m}\text{Lu}$  cross section corresponds to the total radiative capture cross section; (ii) the existence of an unknown long-lived isomer which could trap a part of the  $\gamma$  decay is very unlikely. The goal of this work is (i) to confirm the indirect measurement by a direct detection of the high energy neutrons, (ii) to confirm the high cross section value of the INNA process for the high spin isomer  $^{177m}\text{Lu}$ .

In this paper, we report on experimental results on the direct measurement of high energy neutrons in the reaction between the long-lived isomer of  $^{177}\text{Lu}$  and cold neutrons at the ORPHEE reactor facility. From the previously published value of the INNA cross section and from these measurements, we discuss the relevance of these latter results.

## II. EXPERIMENTAL METHOD

### A. The $^{177m}\text{Lu}$ target

A  $(10.24 \pm 0.01)$  mg natural Lutetium foil ( $25 \mu\text{m}$  thickness) was irradiated at the High Flux Reactor (HFR) at the Laüe Langevin Institute (ILL) in Grenoble (France) to produce  $^{177m}\text{Lu}$  by the radiative capture reaction  $^{176}\text{Lu}(n,\gamma)$ . The V4 port located closed to the core of the HFR was used to take advantage of the maximum neutron flux,  $1.5 \times 10^{15}$  neutrons. $\text{cm}^{-2}.\text{s}^{-1}$ . The natural Lu foil was put inside an aluminium capsule and was irradiated during 6 days. After a 150 days cooling time it was put inside a thin pure aluminium envelop ( $20 \mu\text{m}$  thick). A number of  $(1.03 \pm 0.05) \times 10^{14}$  isomers was accurately measured by performing a gamma-spectroscopy at the time of the measurement performed at the ORPHEE reactor facility. The activity of this radioactive target is 13.22 MBq. A similar non-irradiated natural Lutetium foil from the same natural Lutetium sample used for the isomer target was utilized as a blank target.

### B. The ORPHEE facility

The isomeric target produced at the HFR was moved to the ORPHEE facility in Saclay to perform the experiment. The ORPHEE facility managed by the Léon Brillouin laboratory (LLB) is built around a research nuclear reactor. The 14 MW reactor ORPHEE is made up of a  $56 \text{ dm}^3$  highly enriched in  $^{235}\text{U}$  core, surrounded by heavy water reflector tank to get a good thermal neutron flux  $3 \times 10^{14}$  n. $\text{cm}^{-2}.\text{s}^{-1}$ . Several cold beams are extracted along "neutron guides" emerging from the reactor building. For this experiment, we used the G3.2 point located about 20 m away from the reactor core. The neutron guides are composed of multi-

layered nickel-titanium mirrors and are slightly curved in order to suppress the fast neutrons and gamma-ray background from the core. The internal section of the G3.2 neutron guide is  $25 \times 50 \text{ mm}^2$  giving a neutron flux of  $1.5 \times 10^9 \text{ n.cm}^{-2}.\text{s}^{-1}$  for a mean energy of 4.5 meV and an angular spreading of  $0.4^\circ$ . In order to decrease the background and to increase the detection efficiency, the neutron beam was collimated to a diameter of 2 cm. The collimator shown in Fig. 1, was made up of a sandwich of 0.5 cm thick boron carbide ( $\text{B}_4\text{C}$ ) neutron absorber, followed by a 1 cm thick polyethylene ( $\text{CH}_2$ ) layer and a 2 cm thick lead ( $\text{Pb}$ ) gamma attenuator. It is placed 1.8 m upstream from the target. A second collimator,

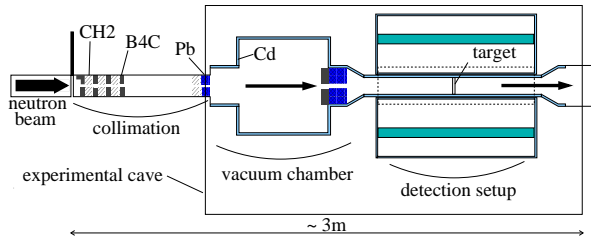


FIG. 1: Setup scheme

made of a 1 cm  $\text{B}_4\text{C}$  and a 5 cm  $\text{Pb}$  layers, is placed 25 cm from the target in order to eliminate neutrons scattered on the first collimator.

### C. The neutron detector

The main difficulty in this experiment is to overcome the low signal to background ratio. Two background sources have to be considered. The first one is due to scattered cold neutrons. To limit this counting rate a dedicated chamber has been built to work under vacuum. The second one is due to photons from neutron captures and the gamma activity of the target itself. The 10 bar pure  $^3\text{He}$  proportional counter from Saint-Gobain company was chosen because of its low sensitivity to gamma-rays. Its outer diameter is 1 inch and its active length is 25 cm. Despite the high photon flux, the neutron detection is unaffected because the deposited energy is small and associated with a very low efficiency. Moreover, the neutron detection is obtained via the exothermic reaction:  $n + ^3\text{He} \rightarrow ^3\text{H} + p$ , whose Q value is 764 keV. Tests with a very intense  $^{60}\text{Co}$  source showed that the thermal neutron peak located at 764 keV was not affected by photon fluxes up to  $10^7 \text{ ph/s}$  on the detector. To detect high energy neutrons, a slowing down neutron counter was used. The neutron array consists of a cylindrical polyethylene moderator combined with twelve proportional  $^3\text{He}$  counters placed inside the moderator. Fast neutrons produced in the target scatter many times in the moderator and quickly slow down by elastic scattering reactions to the thermal neutron energy. under these conditions, the  $^3\text{He}$  detectors have a large efficiency to detect these thermal neutrons. The inner part of the

vacuum chamber is shielded by a 2 mm cadmium layer to suppress the neutrons scattered by the target. An outside 1 mm layer of cadmium covers the whole cylindrical polyethylene moderator in order to stop all thermal neutrons coming from the background or cold neutrons scattered by the collimator. The cadmium layer lets come high energy neutrons into the polyethylene cylinder where they loss their energy. Fig. 2 shows front and side views of the neutron array including dimensions.

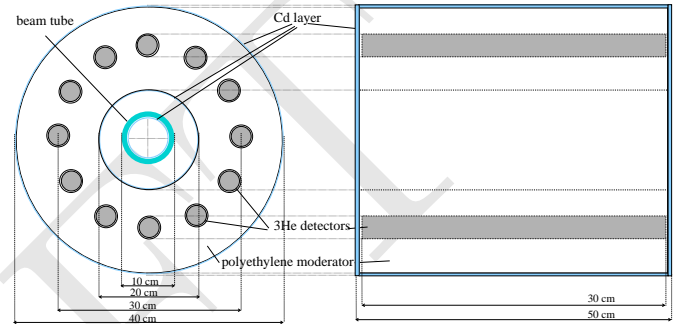


FIG. 2: The neutron detector for the ORPHEE experiment

The neutron array was simulated using MCNP code to get the thermal neutron total efficiency. Emitted neutrons from the INNA process on the isomeric target should strictly have energies up to the isomeric level energy, 970 keV. Looking at the selection rules and the transmission coefficients given in Ref. [9], neutron energies should likely be comprised between 100 keV and 500 keV. The efficiency of the neutron array shown in the Fig. 3 was obtained using the MCNP code [11]. The efficiency in the range of expected neutron energies is flat and is worth 0.198 (see Fig. 3). A very similar response was obtained using the Monte Carlo code GEANT4 [12]. However, our simulation does not take into account the electronic threshold and the wall effect. The correction factor was obtained by measuring and simulating the neutron activity of a known  $^{252}\text{Cf}$  source positioned in the target holder. The  $^{252}\text{Cf}$  spontaneous fission neutron spectrum was simulated through a Watt spectrum with parameters described in [13]. The activity of the  $^{252}\text{Cf}$  source at the time of the experiment was  $(1479 \pm 66) \text{ n.s}^{-1}$  in  $4\pi$ . The source was 18 years old allowing its use without corrections cited in [14]. The corrected detection efficiency to be used is then  $(18.4 \pm 0.9)\%$ .

### D. Neutron flux determination

The neutron flux must be determined at the target position. We used the  $^{175}\text{Lu}$  present in the radioactive target itself to get the neutron flux value at the target position. As the reaction  $^{175}\text{Lu}(n,\gamma)^{176m}\text{Lu}$  takes place during the experiment in the radioactive target, the activation of the  $^{176m}\text{Lu}$  isomer produced by these reactions can be directly used to get the neutron flux knowing the precise amount of  $^{175}\text{Lu}$ . The sample mass was

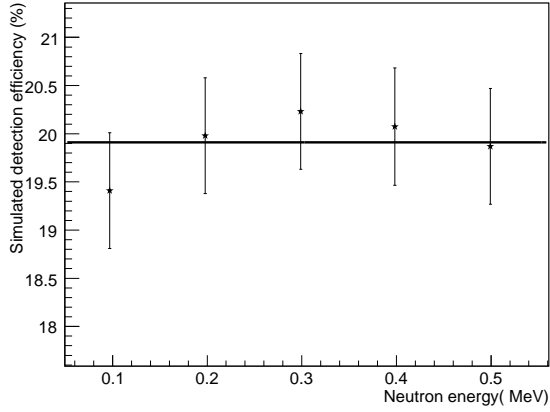


FIG. 3: Detection efficiency of the neutron array obtaining from MCNP simulation. Black line represents the mean value of the detection efficiency.

determined by weighing. From this quantity, the amount of  $^{175}\text{Lu}$  present in the isomeric target could be determined with accuracy knowing the initial  $^{175}\text{Lu}$  quantity, the neutron flux in the V4 port at the ILL high flux reactor and the cross sections of the burn-up of  $^{175}\text{Lu}$ . The burnup correction is 1.75%. The amount of  $^{175}\text{Lu}$ ,  $N_{175\text{Lu}}$ , was obtained to  $(9.80 \pm 0.01)$  mg.

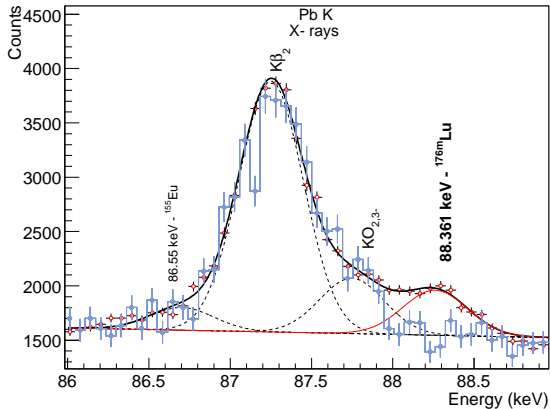


FIG. 4: Gamma energy spectrum of the isomeric target showing the activation of the  $^{176m}\text{Lu}$ . Blue points show data from the isomeric target before irradiation. Red circles represent data from the isomeric target after irradiation.

The activation of the  $^{176m}\text{Lu}$  ( $T_{1/2}=3.664$  h,  $\lambda_{176m\text{Lu}}=(5.25 \pm 0.03) \times 10^{-5}$ ) isomer was measured just after the irradiation at the ORPHEE G3.2 point. A Low Energy Photon Spectrometer (LEPS) was used to measure the 88.361 keV  $\gamma$ -ray from the  $\beta$ -decay of the  $^{176m}\text{Lu}$ . A  $\gamma$  self-absorption correction was applied to this measurement. Fig 4 shows the gamma spectrum of the isomeric target before and after the experiment. The 88.361 keV  $\gamma$ -line clearly appears and its integral  $N_{88\text{keV}}$

is extracted. The reaction rate  $R$  is:

$$R = \frac{N_{88\text{keV}}}{N_{175\text{Lu}}} \times \frac{\lambda_{176m\text{Lu}} \cdot e^{\lambda_{176m\text{Lu}} \cdot t_{ct}}}{(1 - e^{-\lambda_{176m\text{Lu}} \cdot t_{ct}}) \cdot (1 - e^{-\lambda_{176m\text{Lu}} \cdot t_{irr}}) \cdot I_{88\text{keV}} \cdot \epsilon} \quad (1)$$

where  $I_{88\text{keV}}$  is the intensity of the 88.361 keV  $\gamma$ -line and,  $t_{irr}$ ,  $t_{cl}$ ,  $t_{ct}$  are the time of irradiation, cooling and counting, respectively.

The gamma detection efficiency of the LEPS detector located at  $(55.1 \pm 0.5)$  cm was carefully obtained using standard radioactive sources ( $^{133}\text{Ba}$ ,  $^{152}\text{Eu}$  and  $^{241}\text{Am}$ ), and MCNP [11], GEANT4 [12] simulations. This method provides a precise efficiency curve [15]. The efficiency of the setup,  $\epsilon$ , to detect the 88.361 keV  $\gamma$ -ray was determined at  $(2.3 \pm 0.1) \times 10^{-3}$  %.

To extract the flux we need to know the value of the  $^{175}\text{Lu}(n,\gamma)^{176m}\text{Lu}$  cross section in the cold G3.2 flux. The reaction rate  $R$  can be written as:

$$R = \int_0^\infty \phi(\lambda) \sigma(\lambda) d\lambda = \phi_b \cdot \int_0^\infty S(\lambda) \sigma(\lambda) d\lambda \quad (2)$$

where  $\phi$  is the neutron flux ( $\text{n.cm}^{-2}.\text{s}^{-1}.\text{eV}^{-1}$ ),  $\phi_b$  is the total neutron flux ( $\text{n.cm}^{-2}.\text{s}^{-1}$ ),  $\lambda$  the neutron wavelength,  $S(\lambda)$  the G3.2 neutron spectrum previously determined [16] and  $\sigma$  the capture cross section of the beam monitor. Because the cross section in the neutron flux range abides by  $1/v$  law, the integration gives:

$$R = \phi_b \cdot \frac{\sigma_0}{\lambda_0} \cdot \int_0^\infty S(\lambda) \lambda d\lambda = 2.487 \cdot \phi_b \cdot \sigma_0 \quad (3)$$

where  $\sigma_0$  is the  $^{175}\text{Lu}(n,\gamma)^{176m}\text{Lu}$  cross section at  $E_0=0.025$  eV ( $\lambda_0=1.805$  Å), equal to  $(16.7 \pm 0.4)$  barns [17]. The integral value, 2.487, was obtained by a calculation method based on the trapezoidal rule using the curve shown in Fig. 5. In the cold G3.2 flux, the  $^{175}\text{Lu}(n,\gamma)^{176m}\text{Lu}$  cross section is then  $(41.5 \pm 1.0)$  barns.

Finally, using this value and the  $^{176m}\text{Lu}$  activation measurement, we obtain a neutron flux of  $(1.71 \pm 0.16) \times 10^8$   $\text{n.cm}^{-2}.\text{s}^{-1}$  on the target.

### III. MEASUREMENTS AND DATA ANALYSIS

The measurement of the INNA process consists in counting the thermal neutrons detected in the neutron array. Integrals of thermal neutron peaks at 764 keV were extracted for various configurations using the neutron spectrum obtained from the  $^3\text{He}$  detectors. The counting rates were obtained from these integrals. They were corrected for the slight flux variation using the reactor thermal power log file. The counting rate with the neutron beam impinging the Lu radioactive target is  $(4.07 \pm 0.08)$  c/s. The error bar, including statistical and systematic components, is dominated by the latter

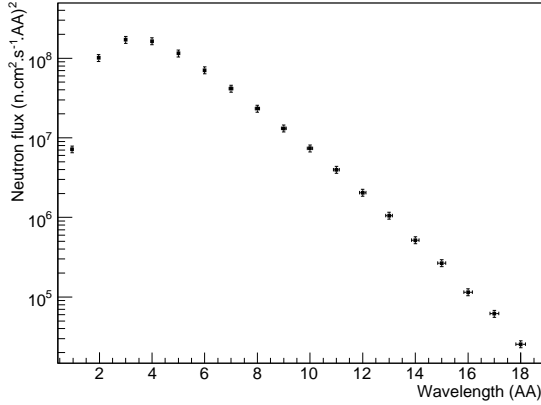


FIG. 5: Neutron flux measured at G3.2 facility [16]

determined by various measurements in similar conditions. All components of the background were detailed and measured: high activity of the target, noise arising from the collimation of the beam, neutron scattering on the target and neutrons from the environment (presence of the reactor, natural radioactivity). In order to determine the contribution of each of these backgrounds, we performed different measurements. The true count of thermal neutrons corresponding to the high energy neutrons is obtained by subtracting all the backgrounds from the full configuration.

TABLE I: Counting rates for various configurations. Beam means that the beam is inside the cave where the neutron detector and the isomeric target are. Beam stop is related to a block made in  $B_4C$  which is just put before the isomeric target letting the neutron beam comes inside the experimental cave. Statistical and systematic errors are reported.

Target	Beam	Beam stop	Counting rate(c/s)
$^{177m}Lu$	on	out	$(4.07 \pm 0.01 \pm 0.08)$
natural Lu 14 mg	on	out	$(2.86 \pm 0.01 \pm 0.08)$
natural Lu 12.2 mg	on	out	$(2.87 \pm 0.01 \pm 0.08)$
natural Lu 6.8 mg	on	out	$(2.79 \pm 0.01 \pm 0.08)$
no	on	out	$(2.565 \pm 0.005 \pm 0.08)$
Al envelop alone	on	out	$(2.637 \pm 0.003 \pm 0.08)$
$^{177m}Lu$	on	in	$(2.690 \pm 0.010 \pm 0.08)$
$^{177m}Lu$	off	out	$(1.139 \pm 0.003 \pm 0.08)$
no	off	out	$(1.21 \pm 0.04 \pm 0.08)$

By analysing of all these configurations, we find that:

- The intrinsic background without beam and isomeric target is  $1.21 \pm 0.04 \pm 0.08$  c/s.
- When the isomeric target is put inside the reaction chamber with no beam, the counting rate is  $(1.139 \pm 0.003 \pm 0.08)$  c/s. No effect coming from the radioactivity of the isomeric target is observed.
- The noise coming from the beam inside the chamber without the isomeric target is

$2.565 \pm 0.005 \pm 0.08$  c/s. This measurement shows that a large part of the background comes from the presence of the beam inside the chamber (mainly from collimators upstream the target position).

- We performed a measurement by stopping the neutron beam in a  $B_4C$  block a few centimeters in front of the isomeric target. The counting rate is then  $2.690 \pm 0.010 \pm 0.08$  c/s. This measurement confirms that the target radioactivity has no influence.
- The contribution of the neutrons scattered on the target was controlled by means of natural lutetium targets surrounded by an aluminium envelop as was the isomeric target. For 6.8 mg, 12.2 mg and 14 mg, the corresponding counting rates are, respectively,  $(2.79 \pm 0.01)$  c/s,  $(2.87 \pm 0.01)$  c/s,  $(2.86 \pm 0.01)$  c/s.
- The influence of the aluminium envelop is determined using an empty aluminium envelop. The counting is then  $(2.637 \pm 0.003 \pm 0.08)$  c/s.

From all these measurements, the systematic error on the counting rate is estimated to be 0.08 c/s. It comes mainly from the imprecision in replacing the sample at the exact target position into the reaction chamber. Tab. I sums up all these counting rates.

Figure 6 shows the response function of the neutron array for these different configurations. The true counting rate of thermal neutrons corresponding to the high energy neutrons is obtained by subtracting all backgrounds from the full configuration. The result obtained is  $(1.20 \pm 0.08)$  neutrons/s.

The observed signal,  $(1.20 \pm 0.08)$  neutrons/s, could be explained neither by the target radioactivity nor the cold neutron scattered by the target. The information gathered in these measurements is summarized by attributing the signal to the INNA process. From the knowledge of the neutron flux, the detection efficiency and the number of  $^{177}Lu$  isomers, the INNA cross-section is  $(363 \pm 48)$  barns.

#### IV. DISCUSSION

This measurement confirms the existence and the high intensity of the superelastic process in the interaction between slow neutrons and the high spin isomer  $^{177m}Lu$ , ( $J^\pi = 23/2^-$ ). In order to compare this value to the INNA cross section obtained in a thermal flux, we have to divide this value by the factor 2.487 as explained above in equation 2. This value,  $(146 \pm 19)$  b, is different from the previously published value  $(258 \pm 58)$  b). This indirect measurement assumes that the neutron capture by  $^{177m}Lu$  can feed neither the  $^{178}Lu$  ground state nor an unknown long-lived isomer which could trap a part of the  $\gamma$  decay. These hypothesis discussed in detail in Ref.[9, 10] and based on physical arguments look to us very reasonable. In contrast, the assumption of the  $1/v$  law to get in equation 3 may be questionable.

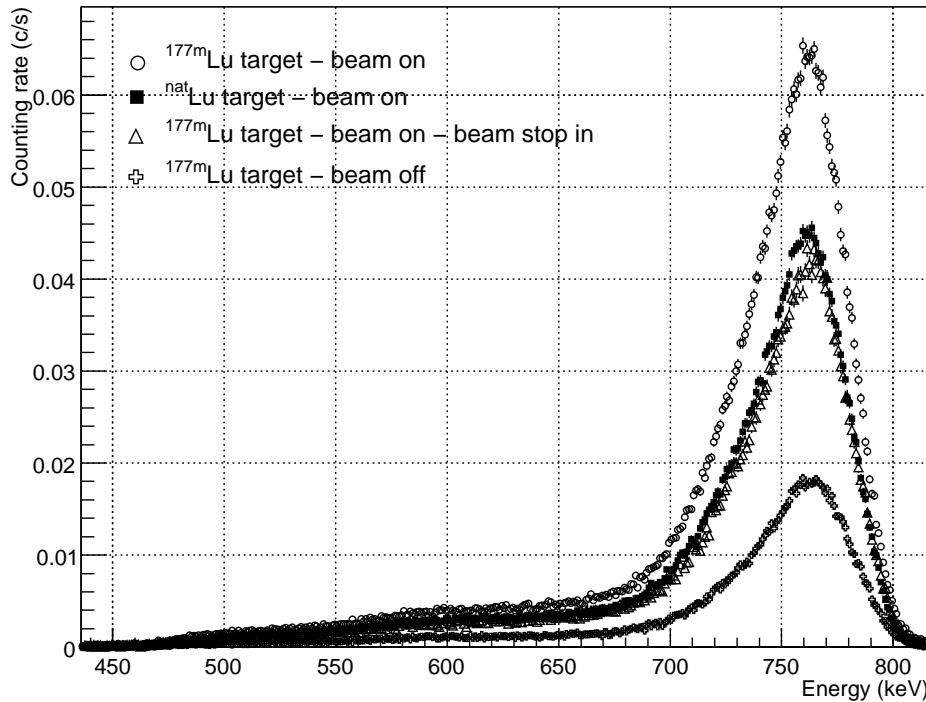


FIG. 6: The signal from the  $^{177m}\text{Lu}$  target and others configurations. Cross curve corresponds to a configuration with the isomeric target and without beam at the target position. Triangle curve is related to configuration with the isomeric target at the target position, with beam stopped by a  $\text{B}_4\text{C}$  block just before the target. Black square curve concerns the 14 mg natural Lu foil at the target position. Circle markers curve is the one showing the full configuration,  $^{177m}\text{Lu}$  target and beam at the target position. Only statistical errors (c/s) are reported here.

Equation 3 assumes that the cross section varies as  $1/v$  law which is not the case for a very low energy resonance. To illustrate this effect, the integrated cross section has been calculated inside a Maxwellian neutron flux at  $T=323$  K and inside the Orphee G3.2 neutron flux. The cross section is described by the Breit-Wigner formula with one isolated resonance. The resonance energy,  $E_R$ , the radiative width,  $\Gamma_\gamma$  and the neutron width,  $\Gamma_{neutron}$ , are adjusted on the Maxwellian averaged radiative capture cross section. The superelastic width,  $\Gamma_{SE}$ , is fixed at 70% of the radiative width as given by thermal measurements [10], [9]. With the resonance parameters given in TAB II, the calculated Maxwellian averaged INNA capture cross section, at  $T=323$  K, is 260 barns compared to  $258 \pm 58$  b, and the calculated Orphee G3.2 cross section is 374 barns, compared to  $(363 \pm 48)$  barns. Figure 8 shows the INNA cross section, the Maxwellian neutron flux ( $T=323$  K) and the Orphee G3.2 neutron flux. The presence of a low energy resonance explains the apparent disagreement between both measurements.

To check whether these resonance parameters are realistic, we performed calculations of their expected average value. Indeed, for such neutron energies the parameters are unpredictable and only statistical distributions

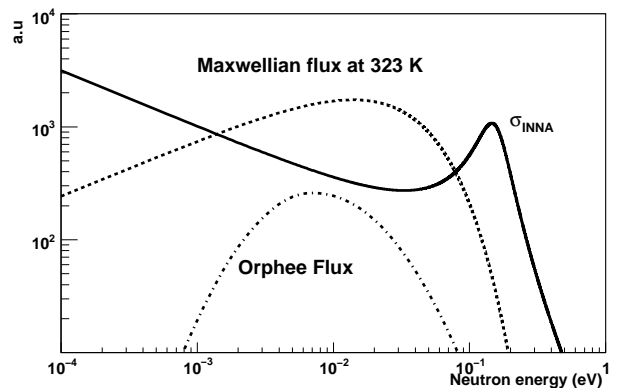


FIG. 7: INNA calculated cross section for  $n + ^{177m}\text{Lu}$  reaction. Black curve is the Breit-Wigner cross section for an isolated resonance with the parameters given TAB II. Dotted curve is the Maxwellian neutron flux at  $T=323$  K and the dashed curve is the Orphee G3.2 neutron flux.

around an estimated value could be calculated.

At low energy the neutron resonance spins are  $11^-$  and  $12^-$ . The averaged level spacing,  $D_0$ , is the inverse

TABLE II: Resonance parameters

$E_R$	0.15 eV
$\Gamma_\gamma$	50 meV
$\Gamma_{neutron}$	$1.8 \cdot 10^{-2}$ meV
$\Gamma_{SE}$	35 meV

of the level density, given here by the Gilbert-Cameron formula. The  $\langle \Gamma_\gamma \rangle$  is determined from the radiative transmission coefficient,  $T_\gamma$ , as :

$$\langle \Gamma_\gamma \rangle = k \frac{T_\gamma D_0}{2\pi} \quad (4)$$

The calculation of the radiative transmission coefficient is based on a  $\gamma$ -ray strength function given by Kopecky and Uhl [18]. The normalization factor  $k$  is adjusted on the known resonance radiative widths of  $^{175}\text{Lu}$  and  $^{176}\text{Lu}$ .

Using the deformed optical potential developed at Bruyeres-le-Chatel, we calculated the S-wave neutron strength function,  $S_0 = 1.98 \cdot 10^{-4}$ . The neutron width is, then, estimated from  $S_0$  by the relation :

$$\langle \Gamma_n \rangle = \sqrt{E_R D_0 S_0} \quad (5)$$

Using the same optical potential, the superelastic width is determined from the neutron transmission coefficients which are calculated for various orbital momenta carried by the emitted neutron [9].

TAB III summarizes the calculated parameters. Compared to the expected average values, the resonance

TABLE III: Expected average value of resonance parameters. The two values for the  $\Gamma_\gamma$  come from the choice of the normalization factor obtained either from  $^{175}\text{Lu}$  or  $^{176}\text{Lu}$

$D_0$	1.4 eV
$\langle \Gamma_\gamma \rangle$	55-95 meV
$\langle \Gamma_{neutron} \rangle$	$10^{-2}$ meV
$\langle \Gamma_{SE} \rangle$	6 meV

parameters given in TABII are in a reasonable agreement. Finally, we have pointed out how such a resonance described by these resonance parameters can be used to understand the disagreement between the cross sections measured in the thermal and cold fluxes. This explanation seems more likely than reconsidering the determination of the radiative capture cross section. The high value of the INNA cross section at very low neutron energy, supported by this direct measurement, shows that this process is very efficient to deexcite a K-isomer. The magnitude of the ratio between the neutron superelastic and the radiative widths, 0.7, means that the overlap between the compound nucleus and nuclear states of the residual nucleus plays a major role. The observation of several low energy neutron resonances built on the  $^{177m}\text{Lu}$  isomer may shed light on nuclear structure at high excitation energy.

## V. CONCLUSION

The inelastic neutron acceleration cross section on the long-lived isomer state of  $^{177m}\text{Lu}$  has been measured in a cold neutron beam. This result although different, confirms the high value of our previous indirect measurement [9]. The observed difference between both values is in favour of the presence of a low energy resonance. This work shows that the interaction of very low energy neutrons with the  $^{177m}\text{Lu}$  is the most efficient mechanism to induce an isomer deexcitation.

## Acknowledgments

The authors wish to express their gratitude to the staff members of the LLB in Saclay, and particularly to Francis Gibert, for their cooperation. Pascal Romain from Bruyres-le-Chatel is thanked for useful discussions and for optical and statistical model calculations on the  $^{177m}\text{Lu}(n,\gamma)$  and  $^{177m}\text{Lu}(n,n')$  reactions.

- 
- [1] Y. V. Petrov, JETP **10**, 833 (1960).
  - [2] I. A. Kondurov, E. M. Korotkikh, and Yu. V. Petrov, JETP Lett. **31**, 232 (1980).
  - [3] I. A. Kondurov, E. M. Korotkikh, Yu. V. Petrov, and G. I. Shuljak, Phys. Lett. B **106**, 383 (1981).
  - [4] Y. V. Petrov and A. I. Shlyakhter, Astrophys. J. **278**, 385 (1984).
  - [5] F. Käppeler, J. Phys. G, Suppl. **s297** (1988).
  - [6] N. Patronis, S. Dababneh, P.A. Assimakopoulos, R. Gallino, M. Heil, F. Käppeler, D. Karamanis, P.E. Koehler, A. Mengoni, and R. Plag, Phys. Rev. C **69**, 025803 (2004).
  - [7] L. Maunoury, P. Delbourgo-Salvador, P. Aubert, J. Aupiais, M. Baudin, G. Bélier, B. Bonnereau, Y. Boulín, F. Pointurier, J.-E. Sauvestre, J. Sigaud and, M. Szmigiél, Nucl. Phys. A **701**, 286c (2002).
  - [8] O. Roig, G. Bélier, J.-M. Daugas, P. Delbourgo, L. Maunoury, V. Méot, E. Morichon, J.-E. Sauvestre, J. Aupiais, Y. Boulín, G. Fioni, A. Letourneau, F. Marie, and D. Ridikas, Nucl. Instrum. Methods. A **521**, 5 (2004).
  - [9] O. Roig, G. Bélier, V. Méot, D. Abt, J. Aupiais, J.-M. Daugas, Ch. Jutier, G. Le Petit, A. Letourneau, F. Marie, and Ch. Veyssiére, Phys. Rev. C **73**, 054604 (2006).
  - [10] G. Bélier, O. Roig, J.-M. Daugas, O. Giarmana, V. Méot, A. Letourneau, F. Marie, Y. Foucher, J. Aupiais, D. Abt *et al.*, Phys. Rev. C **73**, 014603 (2006).
  - [11] J. F. Briesmeister, LA-13709-M, Los Alamos National Laboratory Report (2000).
  - [12] S. Agostinelli, J. Allison, K. Amako, J. Apostolakis, H. Araujo, P. Arce, M. Asai, D. Axen, S. Banerjee, G. Bartrand *et al.*, Nucl. Instr. and Meth A **506**, 250 (2003).
  - [13] A.B. Smith, P.R. Fields, and J. H. Roberts, Phys. Rev.

- 108**, 411 (1957).
- [14] N. J. Roberts and L. N. Jones, *Rad. Prot. Dos.* **126**, 83 (2007).
- [15] K. Jackman and S. Biegalski, *Journal of Radioanalytical and Nuclear Chemistry* **279**, 355 (2009).
- [16] A. Menelle, Private Communication, Léon Brillouin Laboratory (2006).
- [17] S. F. Mughabghab, *Atlas of neutron resonances* (Elsevier Science, 2007).
- [18] J. Kopecky and M. Uhl, *Phys. Rev. C* **41**, 1941 (1990).

DRAFT